



Review

Earth climate identification vs. anthropic global warming attribution[☆]

Philippe de Larminat

Professor (retired) from Ecole Centrale, Nantes, France

ARTICLE INFO

Article history:

Received 3 February 2016

Revised 14 September 2016

Accepted 27 September 2016

Available online 25 October 2016

Keywords:

System identification

Climate

Global warming

Detection and attribution

Anthropogenic

ABSTRACT

Based on numerical models and climate observations over past centuries, the Intergovernmental Panel on Climate Change (IPCC) attributes to human activity most of the warming observed since the mid-20th century. In this context, this paper presents the first major attempt for climate system identification – in the sense of the systems theory – in the hope to significantly reduce the uncertainty ranges. Actually, climatic data being what they are, the identified models only partially fulfill this expectation. Nevertheless, despite the dispersion of the identified parameters and of the induced simulations, one can draw robust conclusions which turn out to be incompatible with those of the IPCC: the natural contributions (solar activity and internal variability) could in fact be predominant in the recent warming. We then confront our work with the approach favored by IPCC, namely the “*detection and attribution related to anthropic climate change*”. We explain the differences first by the exclusion by IPCC of the millennial paleoclimatic data, secondly by an obvious confusion between cause and effect, when the El Niño index is involved in detection and attribution.

© 2016 The Authors. Published by Elsevier Ltd on behalf of International Federation of Automatic Control.

This is an open access article under the CC BY-NC-ND license (<http://creativecommons.org/licenses/by-nc-nd/4.0/>).

1. Introduction

The climatic process is a highly complex system, on which scientists experienced in systems theory have much to say. This concerns particularly the global climate modeling and the attribution of the recent warming to human activity. This analysis involves climatic observations, present and past, direct and indirect. Then, a preferred approach would rely on dynamical systems identification, a theory which is well known to all systems scientists, but has not been applied so far to the climate science.

Actually, bibliographic searches based on the key words *system identification*, *climate*, *global warming*, return strictly nothing related to identification of the climatic process. But if the key words *detection and attribution* are added, there are now dozens of papers regarding the attribution of climate change to human activity. Conversely, the sole couple of keywords *detection and attribution* addresses references exclusively relates to anthropogenic climate change.

In fact, it appears that “Detection and Attribution” (D&A) is an emerging theory, born in the early 21th, dedicated exclusively to

the anthropic attribution of climate change. This last point is clear through the title of the following major publication: “Good practice guidance paper on detection and attribution *related to anthropogenic climate change*”, by Hegerl et al. (2010). The lack of reference to identification is puzzling, knowing that the D&A has close relationships with it, and that the respective findings are mutually inconsistent.

This paper describes the first significant work on the identification of the climate system. It summarizes some findings from our book “*Climate Change, identification and projections*” (de Larminat, P., ISTE/Wiley, 2014). It adds news developments about its relationship with the D&A, and further elaborates on the differences between our conclusions and those of the IPCC.

The latest IPCC Assessment Report is the fifth (AR5, 2013): 1550 pages, 9200 publications quoted. A synthesis is made in the Summary for Policy Makers (SPM, 2013). One of its main conclusions is that “*it is extremely likely that human influence has been the dominant cause of the observed warming since the middle of the 20th century*”. It is mainly supported by Chapter 10 of AR5: “*detection and attribution - from global to regional*”. But these conclusions are infirmed by those based on identification: from the millenary climate observations, it appears that the recent warming is due primarily to natural causes (solar activity and random variations), and that one cannot reject the hypothesis that the human contribution be negligible.

[☆] This research did not receive any specific grant from funding agencies in the public, commercial, or not-for-profit sectors

E-mail address: larminat@wanadoo.fr

The purpose of this paper is to clarify the causes of this contradiction. It is organized as follows.

Section 2 presents the climatic data. Inputs: representative signals of human, solar and volcanic activities; output: the global surface temperature.

Section 3 describes the fundamental features of the Earth's climate system and the mathematical structure of an identifiable model.

The main results of identification are presented in **Section 4**, obtained by the Output Error method (OE), as well as the conclusions of the statistical analysis (reported in appendix) and hypothesis testing.

Section 5 presents and criticizes outcomes of the D&A: first, the observation periods (from a few dozens to about one hundred years) are too short and therefore lead to underestimate the internal variability, increasing the risk of a false detection of the human contribution in global warming.

Furthermore, this recent period is characterized by the simultaneous increase of global temperature and of atmospheric content in CO₂, while the major past climate events (Medieval Warm Period, Little Ice Age) are the only ones that may allow highlighting the solar contribution. Finally, D&A studies which involve the El Niño index make a fundamental methodological error, namely confusion between cause and effect in the climate process. The general conclusions are drawn in **Section 6**.

2. Input-output data of climatic process

2.1. Causes and effects

The Earth's climate is a complex natural system on which we can observe a large amount of signals, among which it is not always easy to distinguish which are causes and which are effects. For systems scientists, the question of causality makes sense only if the concerned system (or subsystem) is clearly delimited; knowing that for coupled systems, the same signal often is both a cause for a subsystem and an effect for another. The answer is unambiguous when the causality can play only in one direction, for example between solar activity and terrestrial climate. It is much less obvious when it comes to variables internal to the climate system, such as the phenomena of oceanic oscillations and the associated ENSO (El Niño South Oscillation) index. We will further comment on this point in **Section 5**.

One of the available means to assess the relative contributions of the different causes is the theory of dynamical systems identification, in particular the branch dedicated to the determination of causal models from observed input output signals. Typical causal dynamic models correspond to linear transfer functions, rational or not, and more generally to state-space models.

Concerning the whole climate system, it is clear that the global temperature is an effect. The major independent causes – on what temperature has no action in return – are the solar activity, the volcanism and, to a large extent, human activities.

The issue of available climate data is crucial, both for identification and for detection and attribution. The reader must therefore get a precise idea of the datasets that we have gathered and used. Knowing the large time scales involved in the climate system, identification requires input-output data whose period widely exceeds those of the 'historical' measures – which, according to climatologists, start between 1850 and 1880. Paleoclimatology allows reconstructing past climate data from substitution measures or proxies (tree rings, isotopes stored in sediments, ice cores, etc.) The accessible reconstructions, available in public data bases (NOAA, NASA, Hadley Center, etc.) are far from overlapping perfectly, and are not always well connected to the historical data.

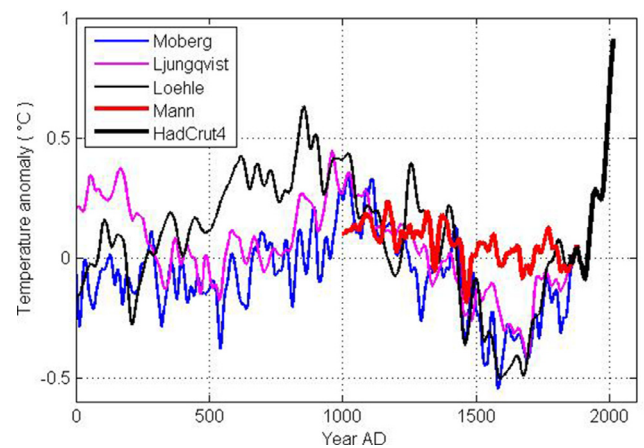


Fig. 1. Four reconstructed temperatures.

2.2. Global mean temperature

As an output, the global climate indicator is the mean surface temperature. Fig. 1 presents a catalogue of four reconstructions: Ljungqvist (2009); Loehle (2007); Moberg et al. (2005); Mann, Bradley, and Hughes, (1999). All four, except Mann, are quoted in the AR5 (Chapter 5: paleoclimate archives). They are aligned on – and extended by – modern measurements from 1850 (HadCrut4: thick black curve).

The further coming back in time, the more rare and inaccurate the proxies are. Some series start at the (symbolic) year 1000. For reasons of accuracy and availability, we will exploit temperatures reconstructions reduced to the second millennium. Moberg and Mann reconstructions are restricted to the northern hemisphere, Ljungqvist and Loehle to extra tropical zones. Nevertheless, the differences between modern temperatures of the northern and southern hemispheres are much lower than the observed disparities between the reconstructions above, which allow considering that the North/South or other climatic differences are dominated by errors due to proxies and reconstruction techniques.

We note that the curve of Mann, called *Hockey Stick Graph*, deviates significantly from others, which will reflect on the results of the identification.

2.3. Anthropic indicator: CO₂ atmospheric concentration

Human activity has an impact on the emissions of greenhouse gases (GHG), industrial aerosols, land use changes, etc. From C, the atmospheric concentration of CO₂, we define a global indicator of human activity as:

$$u_1 = \log_2(C/C_0)$$

where C₀ is the preindustrial concentration (*ante* 1750), about 280 ppm (*parts per million*).

Several reasons motivate this formula. First, the action of CO₂ is reportedly predominant. Also, others anthropogenic actions are cross-correlated and may tend to mutually compensate. Moreover, the CO₂-induced greenhouse effect is widely admitted to follow a logarithmic law. Finally, CO₂ doubling is often considered as the unit of variation; hence the interest of the base 2 logarithm.

Fig. 2 shows the signal u₁, resulting from the connection of modern atmospheric measures with the archives extracted from Arctic or Antarctic ice cores (source: NOAA and CDIAC). Note that $u_1 = 0.5 \leftrightarrow C = C_0 + 41\%$

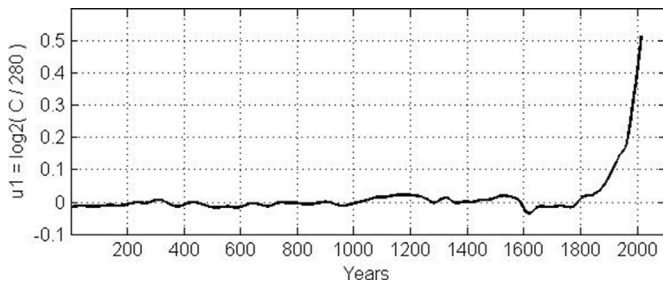


Fig. 2. Anthropic signal: $u_1 = \log_2(C/C_0)$.

2.4. Solar activity

The manifestations of solar activity are multiple and likely to impact the climate through extremely various mechanisms.

1. First of all, there is obviously the total energy flux (TSI: Total Solar Irradiance), weakly variable around 1367 Wm^{-2} , and which directly affects the Earth's radiative balance.
2. The IR/UV spectral distribution acts differently, through the stratospheric creation of a GHG (the ozone).
3. The solar magnetism modulates cosmic radiations, which are likely to act on the formation of condensation nuclei and thus on terrestrial cloud cover and its albedo effect. This modulation is found in proxies consisting of cosmogenic isotopes (or cosmoneutrons: ^{12}Be , ^{14}C).
4. The solar wind, and its known role in boreal Auroras.
5. The background radio noise, not or little studied in the climate context...

All the signals related to solar activity clearly appears as a sum of three components: (1) cyclic, period around 11 years, (2) high-frequency (HF), (3) low-frequency (LF). For example, Fig. 3

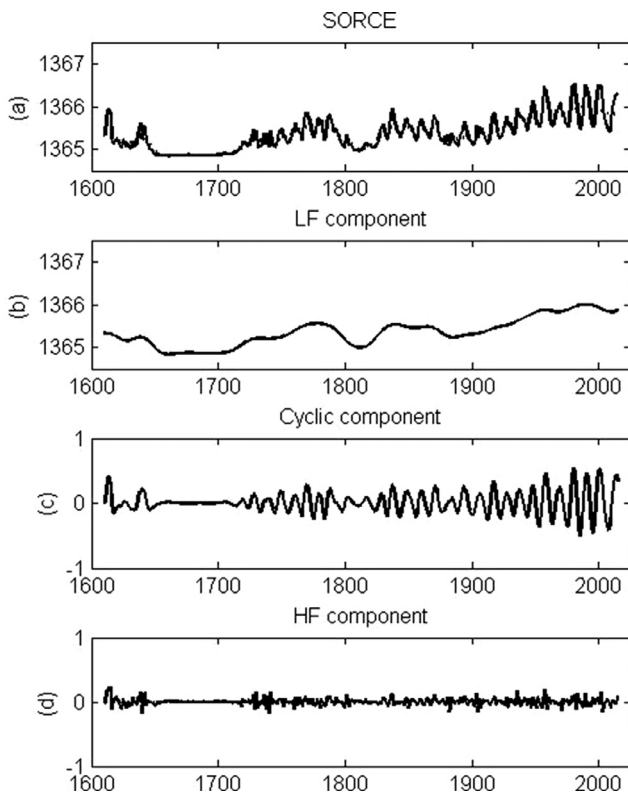


Fig. 3. SORCE/TIM decomposition.

shows the 3-components decomposition of the TSI reconstruction SORCE/TIM (Solar Radiation and Climate Experiment/Total Irradiance Monitor) by Kopp and Lean (2011). This composite reconstruction is based both on modern satellite measurements and on sunspots observed since 1610 (invention of the Galileo telescope). Our decomposition principle is outlined in annex A.

In all signals and proxies related to solar activity, one can find, with different relative magnitudes, the same cyclic component and the same LF component (HF component being widely considered a measurement noise). The mutual ratio between the cyclical and the LF components is extremely variable, depending not only on the nature of the signals (associated to mechanisms 1 to 5 above), but also on the given reconstructions of a same signal, in particular the TSI.

The cyclic components of all the TSI reconstructions have indeed roughly the same maximum excursion (1 Wm^{-2} in the 20th century), but from 17th to 20th, according to reconstructions, LF components range from 1 to 10 Wm^{-2} (see, for example, Lean (2004) or Shapiro et al. (2011)). These differences come from the absence of TSI measures over sufficiently long periods allowing calibration with a good precision of the LF components of proxies related to solar activity.

On the other hand, it is recognized that the cyclic variations (11 years) detectable on the global temperature are practically negligible (less than one-tenth of degree). If we admit that the reconstruction SORCE/TIM is valid and that solar activity occurs on the climate exclusively through the energy factor (mode 1), we should conclude, like IPCC does, that the impact of solar activity is almost zero.

Some mechanisms involved in low-frequency (through the heliocentric magnetic field, for example) are not yet well enough understood to include them in the physical models. It does not imply that they do not exist. Our identification is precisely intended to determine if the climatic contributions of the low-frequency solar activity is significant, if not predominant.

If therefore one accepts either that LF variations of TSI can be very superior to those of Fig. 2, or that other mechanisms of solar activity may predominate over the energy factor, the just way to highlight it will be to restrict reconstructions and/or proxies of solar activity to their only LF components.

2.5. Low Frequencies indicators for solar activity

Given the multiplicity of manifestations and mechanisms of solar activity, there would be no reason to favor one physical signal rather than another (TSI, heliocentric magnetic field, potential solar modulation...), or one proxy in preference to another, especially after reduction to low frequencies component.

For various needs, it is however preferred to convert everything in terms of TSI. We arbitrarily adopted here for reference signal the SORCE/TIM reconstruction, widely used by IPCC (AR5), and limited here to its LF component (Fig. 3-b). After calibration and alignment on this component, Fig. 4 combines the LF components of the four following proxies:

- The SORCE/TIM LF component itself.
- The series of sunspots groups number (SGN), reconstructed since 1610, recently reviewed and corrected by the Royal Observatory of Brussels (Clette, Svalgaard, Vaquero, & Cliver, 2015).
- The cosmogenic series of Usoskin, Korte, and Kovaltsov (2008), initially expressed in CR11 (Cosmic Ray Induced Ionization Rate Reconstruction), based on concentrations of ^{14}C (years 5 to 2005).
- The cosmogenic series of Delaygue and Bard. (2010), initially expressed in ^{10}Be anomalies (years 695–1982).

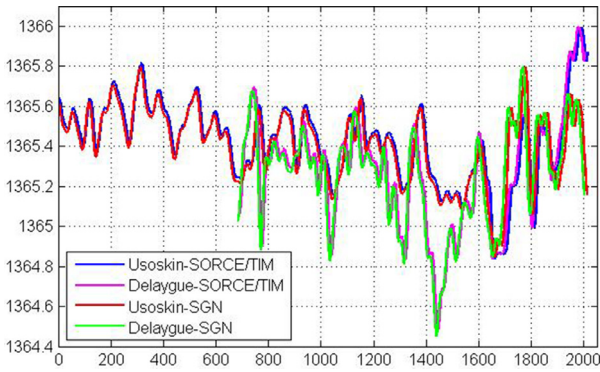


Fig. 4. Four low frequency index for solar activity.

Making connections Usoskin-SORCE/TIM, Delaygue-SORCE/TIM, Usoskin-SGN, Delaygue-SGN, this produces a catalogue of four solar indicators (Fig. 4).

2.6. Volcanic activity

Volcanic activity is estimated through the Aerosols Optical Depth (AOD) produced by eruptions (Crowley & Unterman, 2013).

Fig. 5 shows this indicator u_3 , centered on its mean value and sign changed, because volcanism is known to impact the temperatures downwards.

3. An identifiable model

3.1. General circulation models (GCM)

GMC's are knowledge models, which can be simulated by finite elements, including thousands of interconnected cells (atmospheric and oceanic). The equations that govern each cell and their mutual interactions are firstly those of fundamental physics: mass and energy conservation, fluid mechanics, thermodynamics, radiation, etc.

They incorporate also some amount of more or less empirical representations concerning for example the clouds, their genesis and their radiation and absorption properties, or the heat transfer at the Earth's surface by convection, evapotranspiration, etc. The associated parameters are somewhat arbitrary and usable as adjustment variables. The overabundance of adjustable parameters gives designers the ability to get any desired result, in particular accurate reproduction of the warming in the last quarter of XXth century.

Note finally that the GCMs spontaneously reproduce the fluctuations of the atmospheric or oceanic chaos, at the origin of the climate internal variability (see Section 3.6).

3.2. Energy balance models (EBM)

The large numerical models are obviously the only ones able to reflect the regional climatic particularities. However, if interest is primarily focused on global behaviors, the climate system makes no exception to the vast majority of complex systems, which lend themselves to representation by input-output models, so-called 'black box' (or 'grey box' models, when they incorporate some macroscopic physical laws).

This is the case of so-called Energy Balance Models, some of which have been developed by IPCC (e.g. Meinshausen, Raper, & Wigley, 2011). These models reproduce the global behavior of large digital models, on which they are tuned, but their complexity is not yet reduced enough to make them identifiable from the available input-output climate observations.

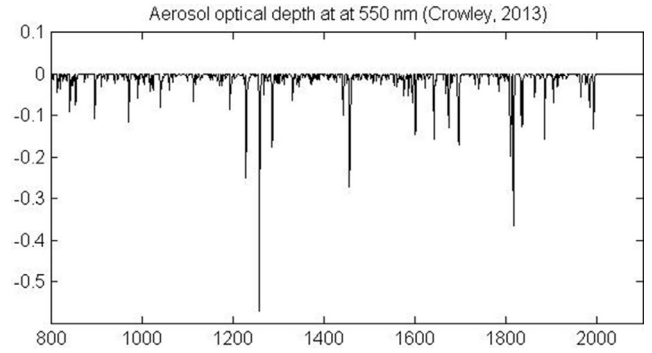


Fig. 5. Volcanic activity.

3.3. Proposed structure

Our climate model is organized into two coupled subsystems (Fig. 6).

The *heat accumulation* subsystem includes all the thermal inertia in which the flow Φ of energy balance (in Wm^{-2}) accumulates, circulates and diffuses. It mainly consists in oceanic mass, the superficial thermal inertias of the continents being negligible.

The thermal inertia of the atmosphere is also negligible. It accumulates virtually no energy, so that the radiative balance Φ at the Top Of the Atmosphere (TOA) is therefore fully transmitted, without significant delay, into the oceanic thermal inertia. Immediacy is to be understood here with respect to the climate time scale, i.e. less than one year (time unit adopted in climatology).

The *thermal exchanges* between atmosphere, ocean and space are driven by the three aforementioned independent causal inputs u , referred to as forcing factors, and also by the resulting global surface temperature T_G , which depend itself on the oceanic temperature T_O .

3.4. Mathematical expression of the model

The accumulation of heat in the oceanic thermal inertia is described by:

$$I_O dT_O/dt = \Phi \tag{1}$$

where I_O is in $(W/m^2)/(K/year)$.

The *thermal exchanges* (Fig. 6) expresses into algebraic equations. Regardless of their complexity, one can admit the existence of linear approximations. Then, Φ is classically written as:

$$\Phi \approx \alpha_1 u_1 + \alpha_2 u_2 + \alpha_3 u_3 - \lambda (T_G - T_E) \tag{2}$$

Recall that the u_i are the deviations of the forcing indicators compared to their nominal values. The products $\alpha_i u_i$ give the resulting radiative forcings, where the α_i 's are the associated coefficients of radiative forcing.

T_E is the hypothetical surface temperature at equilibrium, when $u_1 = u_2 = u_3 = 0$, and assuming the absence of internal variability.

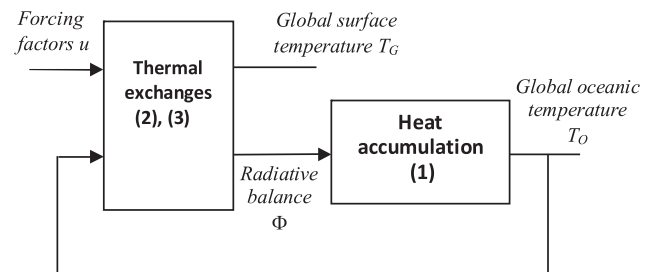


Fig. 6. Structure of an energy balance model.

This T_E is unknown, due to the lack of measurements in the pre-industrial era.

λ is a climatic feedback coefficient, expressing the variation of the radiative balance under the effect of the deviation $T_G - T_E$. All the above parameters are widely used in the climate science. They directly result from the universally accepted concept of energy balance.

In (2), the global surface temperature T_G results from the thermal version of the Ohm law:

$$T_G = T_0 + r \Phi \quad (3)$$

where r denotes the thermal resistance through the surface, depending on the convection characteristics of the atmospheric and oceanic limit layers, and on the evapotranspiration properties of the surface. Eliminating Φ between Eq. (1 to 3) easily leads to the monodimensional state space model:

$$\begin{aligned} T_{\text{clim}} dT_0/dt &= -T_0 + T_E + \sum S_i u_i \\ T_G &= (1 - \rho)T_0 + \rho T_E + \rho \sum S_i u_i \end{aligned} \quad (4)$$

where:

$$T_{\text{clim}} = I_0 (1 + r\lambda)/\lambda, \quad \rho = r\lambda/(1 + r\lambda), \quad (5)$$

$$S_i = \alpha_i/\lambda, \quad i = [1 : 3] \quad (6)$$

An equivalent formulation is the following:

$$(T_G - T_0) = G(s) (S_1 u_1 + S_2 u_2 + S_3 u_3) \quad (7)$$

where

$$G(s) = \frac{1 + \rho s T_{\text{clim}}}{1 + s T_{\text{clim}}} \quad (8)$$

is a transfer function of unit dc gain ($G(0)=1$) and the S_i 's are the equilibrium sensitivity coefficients with respect to the forcing factors u_i .

The structure (7, 8) results from reasonable physical assumptions. The most important point is that the transfer function $G(s)$ is common to the three entries. This comes from the fact that the radiative balance is generated by the atmospheric machinery, assuming a negligible thermal inertia, and therefore modeled by algebraic equations, such as 2 and 3. The transfer function $G(s)$ reduces here to a first-order filter (with numerator), which appears to be sufficient to describe the climatic transients in response to the low frequency components of the excitations u_i . It is not necessary to introduce a transfer function $G(s)$ of higher order, as we did in our book (de Larminat, 2014). Even without formal evaluation (AIC criterion, for example), it appears through our identification attempts that higher order models are over-parameterized, regarding the input output data, which would require – as we previously did – an arbitrary tuning of the denominator the denominator of $G(s)$, in order to reduce the number of free parameters.

3.5. A priori estimates

The model will be identified under the reduced form (7, 8). In its last report, IPCC gives bounds for equilibrium sensitivity to CO₂ doubling:

$$1^\circ\text{C} < S_1 \text{ (Prob. } > 95\%), \quad S_1 < 6^\circ\text{C} \text{ (Prob. } > 90\%) \quad (9)$$

IPCC does not directly provide such bounds for the solar sensitivity S_2 . Nevertheless, we can deduce it, knowing that (6) implies $S_2 = (\alpha_2/\alpha_1) S_1$. According to IPCC, the radiative forcing to CO₂ doubling is $\alpha_1 \approx 3.7 \text{ Wm}^{-2} \pm 10\%$. In the IPCC models, solar activity is assumed to be acting through the energetic factor only, then $\alpha_2 = 1$, after converting the TSI into Net Solar Irradiance: $\text{NSI} = (1 - 0.3)/4 \times \text{TSI}$, where the factor 1/4 is for Earth sphericity

and where 0.3 is the mean terrestrial *albedo*. Dividing (9) by α_1 , we obtain the following bounds on sensitivity irradiation:

$$0.27^\circ\text{C/Wm}^{-2} < S_2 < 1.62^\circ\text{C/Wm}^{-2} \quad (10)$$

Using our solar indicators, based on *SORCE/TIM*, we shall see that the identified lower bound for S_2 will be much greater than the above upper bound, except when using the hockey stick curve.

3.6. Internal variability

The *natural variability* of the climate results from variations of causes other than human (solar, volcanic). It includes also, but is not restricted to *internal variability*, which mainly comes from turbulences, inherent to any fluid flows. The chaos of the atmospheric and oceanic circulations originates from a tingling of independent causes: the famous flaps of butterfly's wings, able to initiate – or not – meteorological or climatic events). Globally, internal variability is equivalent to an additive disturbance v acting on the output:

$$(T_G - T_0) = G(s) \sum [S_i u_i] + v$$

This disturbance is not a white noise (an independent sequence) and its spectrum will be taken into account, if not in the method of identification, at least in the calculation of the variance of the estimated parameters (see Appendix B).

4. Identification

4.1. Specificity of the climate process identification

In system identification, it is usually recommended to save part of the data for model validation purposes. To do this, it would be necessary, either to have multiple experiments, or to split a single one, but of long duration.

History, climate or other, does not repeat itself. Regarding the low frequencies involved in the climate process, one millennium is barely enough, and splitting would make it unusable for the identification, in particular with regard to solar activity. In this situation, validations through the statistical calculation of the uncertainty ranges according to rigorous methods is therefore of particular importance.

Another difficulty comes from the discrepancies in the reconstructions of temperature and of solar irradiance (Figs. 1 and 4).

Depending on the selected data, some uncertainty ranges will reveal incompatible with each other (see below Fig. 10). In absence of objective criteria for rejecting some data rather than others, the only objective attitude is to present all of the results obtained from the 16 possible combinations (4 temperature \times 4 solar irradiances), and to leave observers their freedom of judgment.

4.2. Method

Since several decades, identification of dynamic systems is a mature discipline: Åström and Eykoff (1971); de Larminat and Thomas (1977); Söderström and Stoica (1988); Walter and Pronzato (1997); Ljung, (1999); de Larminat (2009), chapter 13; Landau (2001).

Here, observation data are poor in events and severely disturbed by noises and internal variability. Then, the simplest and most robust method is the Output Error method (OE).

The principle is easily understandable, even by non-experts: it consists in simulating the model (here the Eq. (7)), fed by the recorded input signals u_i , and in tuning the parameters of the model until the deviation between the simulated and observed output be minimized in the mean square sense. Using the OE method, the observation data speak freely, without any constraints

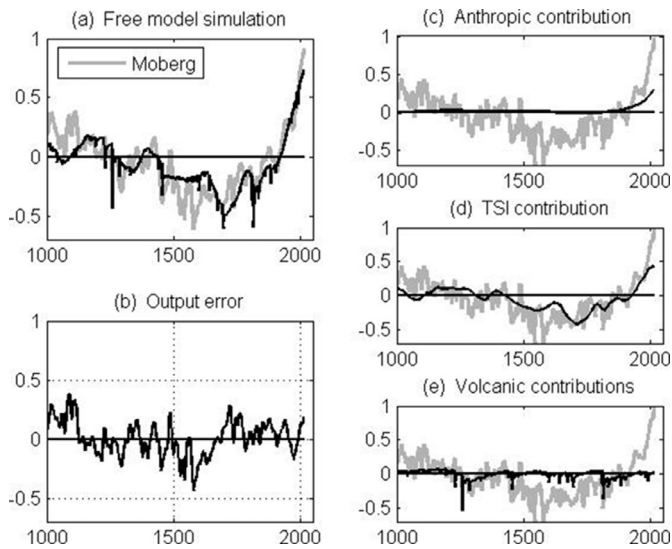


Fig. 7. Free identification.

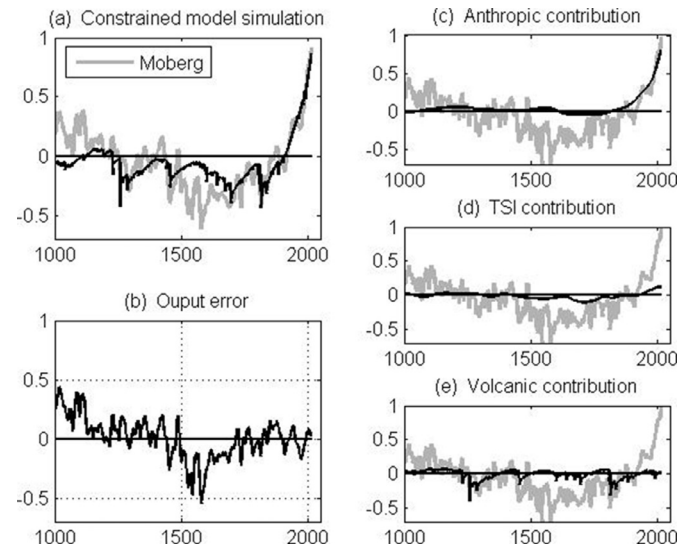


Fig. 8. Constrained identification.

that could impact the results, nor even structures or variances of noises.

Actually, like for many other identification methods (AR, AR-MAX, B&J, PEM, etc., see Ljung (1999)) the statistical characteristics of the noises and disturbances are extracted from the observed data themselves (here from the correlation function of the residuals). So, we do not need to make use of the confidence ranges that are often provided with the climate data.

In our case, the residual output error will be far from a white noise (Fig. 7-b). The method is therefore not statistically optimal. This does not prevent computing the variance of the estimator (under the classical approximations: normality, ergodicity, asymptotic convergence, etc.) See Appendix B.

4.3. First set of results

Consistently with our principles, we have dealt with all the combinations of data sets, but for the sake of illustration, this section is limited to the identification results from our first combination of temperature and irradiance, namely Moberg \times Usoskin-SORCE/TIM.

Fig. 7 shows (a) the simulated output of the optimized model, (b) the output error and (c, d, e) the respective contributions of the three forcing factors. In these frames, the light grey curves show the observed output (Moberg).

It can be seen that the output error is large, but comparable with the millennial simulations of IPCC (see e.g. AR5, 2013; Fig. 1 (b), p. 78). This comes not only from output noise, reconstruction errors, and identification errors, but mainly from the internal climate variability (Section 3.6), irreducible by nature. This last component being not a white noise, it not an independent identically distributed sequence (idd).

Yet in this first case, the recent anthropogenic contribution is found to be less than the contribution of solar activity. Reflecting the predominance of internal variability in the error output, the natural contribution (solar and volcanic activities, plus internal variability) becomes clearly much greater than the anthropogenic contribution in the recent warming.

Recall that the contributions shown in Fig. 7 are specific to our first combination of data. One should therefore not yet generalize these conclusions.

4.4. Tests of hypothesis

Another way to practice the identification techniques is to perform forced optimizations, under assumptions of which we want to test the relevance. According to the IPCC, solar activity acts exclusively through the total flux of solar irradiance, with a rather insignificant solar sensitivity, most likely less than $1.6 \text{ } ^\circ\text{C}/\text{Wm}^{-2}$ (Eq. (10)).

As expected, performing the identification under this constraint ($S_2 < 1.62 \text{ } ^\circ\text{C}/\text{Wm}^{-2}$) leads to an insignificant solar contribution (Fig. 8-d), and recent warming mostly attributed to the anthropic factor (frame c).

Some indications tend to dismiss this hypothesis:

- In the free identification, solar activity contributes to explain the medieval warm period and the little ice age. It is not so in forced identification (Fig. 9-d).
- As a result, the error output visibly increases over these periods.
- A significant cross-correlation (not shown here) appears between the solar activity indicator and the output error, sign of a causality not taken into account.

Visual assessments being not formal proofs, this must be confirmed by hypothesis testing, in order to confirm whether the error output really significantly increases, implying rejection of the hypothesis. The statistical tests, based on the estimated variances (Appendix B) show that: *the hypothesis of a low sensitivity to solar activity must be rejected with a probability level greater than 90%*.

Similarly one can test the hypothesis of a low anthropogenic sensitivity, in the limit $S_1 = 0$. Then, the reproduction of recent warming is significantly degraded, but the estimated internal variability remains comparable to the millennial values. The hypothesis test confirms: with a 90% probability level, one cannot reject the hypothesis of a zero anthropogenic contribution. In other words: *The selected combination of observation data invalidates the claim of the IPCC, that the anthropogenic contribution to recent warming is predominant with 95% probability level.*

4.5. Exhaustive results

Previous results were one-off, based on one particular set of data. Instead of detailing similar results, contributions and tests

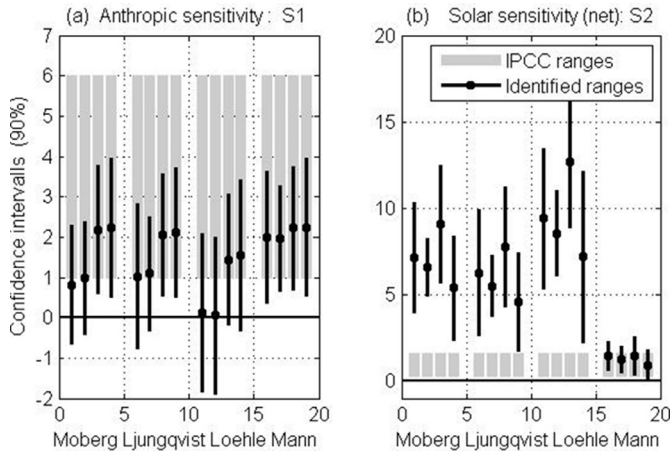


Fig. 9. Confidence intervals.

relating successively to each set, Fig. 9 limits to the estimates of S_1 and S_2 , along with their 90% confidence intervals, calculated from the 16 combinations of data. There are grouped into four sets, relating to the respective reconstructions of Moberg, Ljungqvist, Loehle and Mann. Each group is subdivided according to the four reconstructions of solar irradiance (Section 2.5). The grey segments show the ranges of sensitivity according to IPCC (Eqs. 9 and 10).

Fig. 9-b clearly shows a total mismatch between confidence intervals resulting from the use of the Mann's reconstruction and those from the first three. At the same time, this last alone could confirm the IPCC parametric ranges, both for the anthropic and the solar sensitivity.

At the outset, there is no reason to discard the reconstruction of Mann: scientific truth does not determine by majority. The hockey stick graph had appeared repeatedly in previous reports of the IPCC, and it is still widely used in many vulgarization reports on climate change. But one cannot ignore that it has been the subject of serious controversies; and it must also be reported also that the IPCC no longer mentions it anywhere in the 1550 pages of his 2013 report, even in chapter 5 on Paleoclimate Archives.

If we limit ourselves to the three other reconstructions (Moberg, Ljungqvist, Loehle), then our conclusions are as follows:

About anthropic sensitivity:

The partial conclusions of 4.3 and 4.4 don't generalize. In the whole, the lower bound $S_1 > 1^\circ\text{C}$ can neither be confirmed, nor invalidated. It depends also of the TSI reconstructions. But in all cases, the upper bound $S_1 < 6^\circ\text{C}$ is far from being reached.

About solar sensitivity:

The first three reconstructions lead to reject the IPCC hypothesis of a low sensitivity to solar activity.

Two explanations may combine. The first could be the existence of mechanisms of solar action other than energy factor, the only one retained by IPCC; the second could be a too low evaluation assessment of the LF component in the SORCE/TIM reconstruction, used as reference in Section 2.5. If one adopts a reconstruction where the LF component is higher, such as Shapiro et al., (2011), then the identified sensitivity range might become comparable with that of the IPCC.

Now, the most important is not the value of the coefficient S_2 , but the assessment of whether or not the contribution of natural factors prevails on the human contribution. In Fig. 10, twelve simulations (discarding again those from Mann) show the anthropogenic contributions on the last century. On average, the assertion of the IPCC that most of the warming observed during the second half of the 20th century is of human induced is not confirmed.

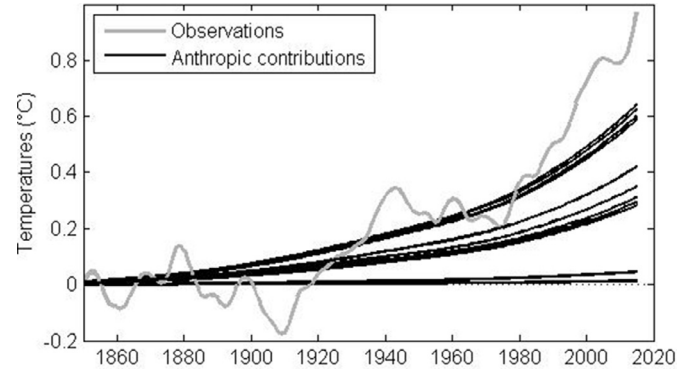


Fig. 10. Anthropogenic contribution to climate change.

For further investigations, it would be of interest to use more refined analyses, for instance (Faivre, Iooss, Mahévas, Makowski, & Monod, 2013).

Anyway, one can think that the above conclusions are robust: they remain practically the same as in our previous works (de Larminat, 2014), despite substantial quantitative changes, consecutive to the structure adopted for the model, the frequencies decomposition of solar activity and the selected paleoclimatic data.

5. Detection and attribution

5.1. Introduction: "Good practice guidance paper on detection and attribution" (GPGP)

Generally speaking, detection recognizes if there actually exists a phenomenon potentially masked by random fluctuations; while the attribution specifies, or even quantifies the causes to effect relationship. D&A operates on the basis of climate observations and from some predetermined climatic models (GMC or EBM). Unlike identification, it does not intend to rebuild or to retune these models. Note that the human-induced climate change is set as a principle. This appears in the complete title: "Good practice guidance paper on detection and attribution related to anthropogenic climate change" (Hegerl, 2010), which echoes the mission of IPCC: "assess the scientific, technical and socio-economic information relevant for the understanding of the risk of human-induced climate change." (www.ipcc.ch/Procedures/Principles/Role).

This 'Good Practice Guidance Paper' (GPGP), was intended for the drafters of the future AR5 report being prepared at that time. GPGP is partly a compendium of definitions and language elements: it specifies that *external forcing* refers to causes external to the climate system seen as a whole (typically human, solar and volcanic actions), while the term *external drivers* is for more general use (e.g., 'the reduction of sea ice might act as an external driver on polar bear populations').

It also introduces the concept of *confounding factor* "which may mask or shears the effects of external forcings and drivers". A long list includes the following items: "...model errors and uncertainties; improper or missing representation of forcings in climate and impact models; structural differences in methodological techniques; unaccounted or unaccounted for internal variability...". Each of the points above would have deserved further clarifications: by itself, warnings against confusions do not ensure that the D&A provides adequate tools to avoid them. In particular, "unaccounted for internal variability" is mentioned as one such confounding factor. Actually, it seems at the contrary that it is *accounting for ENSO index* which would constitute an obvious confusion, this between cause and effect (Section 5.5).

GPGP lists various methods for D&A: attribution to external forcings (single-step or multi-step: depending on whether the

chain of causality is single or multiple); associative pattern attribution; assignment to a change in climatic conditions “which may be the final step in Multi-Step Attribution”. This last mention is important: the GPGP points out that ‘the overall assessment will generally be similar to or weaker than the weakest step’.

The SPM describes about twelve climatic effects, all attributed to anthropogenic influence: in the first place the global warming itself. Then, come the melting of sea ice, the raising of the sea level, the frequency of extreme events, the heat waves, etc. In chapter 10 of AR5, about sixty contributors provide dozens of other examples, giving material to about 700 bibliographical references. However most of the submitted attributions are multi-step ones and involve anthropic global warming as an initial step. If the weakest link lies in the attribution of global warming to human activity, then the reality of all these attributions becomes highly questionable, and their accumulation cannot in any way be considered as multiple evidence of human influence on climate.

Subsequently, we will thus focus exclusively on the assessment of the validity of the attribution of global warming by mean of the D&A.

5.2. D&A and fingerprinting

One of the main tools used in D&A is called ‘optimal fingerprinting’, a concept introduced in the 1990’s (Hasselmann, 1993). The principle is as follows (see, for example, Hegerl and Zwiers 2011).

Regarding global temperature, fingerprints (or patterns) are defined as the changes in the simulated temperature in response to observed variations of each external forcing or driver, considered independently. The used simulation models are either some large digital general circulation models (GCM), either simple energy balance models. Unlike the approach of identification, these models are *a priori* fixed, and the D&A is not intended to revisit them. Making explicit linear hypothesis:

$$y = X_1 + X_2 + X_3 + v \quad (12)$$

where y is the observed global temperature, X_i the fingerprints associated with each indicator of forcing (e.g., human, solar and volcanic activities), and v results from internal variability or from any unlisted causes. Introducing possible model errors, Eq. (12) becomes:

$$y = Xa + v \quad (13)$$

where $X=[X_1 X_2 X_3]$, and where a is a vector of scaling factors, each nominally equals to 1. An estimate of a may be obtained by some linear regression (e. g. BLUE: Best Linear Unbiased Estimate):

$$\hat{a} = (X^T C^{-1} X)^{-1} X^T C^{-1} y \quad (14)$$

where the matrix C is the covariance of internal variability signal, the determination of which we will return on. The variance of the estimate \hat{a} is given by the expression $(X^T C^{-1} X)^{-1}$, from which one can deduce the confidence intervals associated with estimates \hat{a} . Depending on whether the estimated intervals include (or not) the values 1 or 0, changes in y will be detected (or not), and will be attributed (or not) to the corresponding forcing factor.

5.3. Relations with identification

The D&A allows involving the large General Circulation Models, and thereby addressing regional or local phenomena, ignored by the ‘black boxes’ models. But if one restricts to the fundamental question of the attribution of global warming, the D&A is strongly related with our identification, so much that both methods might be expected to lead to the same conclusions.

Actually, let’s take again our model structure (Eq. 7): $(T_G - T_0) = G(s) (S_1 u_1 + S_2 u_2 + S_3 u_3)$. The associated fingerprints are

then nothing else than the contributions of the various inputs to the output, simulated by a model fully specified *a priori*, including $G(s)$ and sensitivities: $X_i = G(s) S_i u_i$.

Then, the vector \hat{a} , obtained by optimal fingerprinting (Eq. 14) would allow a readjustment of the initial sensitivities, by multiplying the *a priori* given values S_i by the factors \hat{a}_i . The main difference between our identification and D&A is that the last kept the transfer function $G(s)$ outside the scope of the identification. In the GCM, the sensitivities do not appear explicitly. The D&A therefore cannot lead to identification strictly speaking. Besides this point, there is no fundamental difference in nature between deductions based on D&A and those from system identification, by hypothesis testing’s and confidence intervals.

By nature, this identification has the advantage of taking into account uncertainties on the transients modeled by the $G(s)$, while the D&A only claims being robust: “Attribution does not require, and nor does it imply, that every aspect of the response to the causal factor in question is simulated correctly” (AR5, p 873). If one admits this, it is therefore necessary to look elsewhere to understand why the conclusions between D&A and identification are so much opposed. Minor technical differences, such as OE vs. BLUE do not bring significant explanations. Ultimately, the explanation would first of all be in the data used, their period and their natures.

5.4. Observation periods

Almost all of D&A studies focus on climate observations starting after 1850, sometimes even well afterwards (1979). These durations are much too short.

A first reason lies in estimation of the statistical characteristics of internal climate variability (the C matrix of Eq. (14)), which is essential to detect whether a variation emerges or not above the level of internal variability. This variability can be first assessed by means of general circulation models simulations, which inherently can reproduce the atmospheric and oceanic chaos, primary responsible for internal variability. Then it raises the question of the ability of these models to actually reproduce the variance and especially the low-frequency spectrum of this variability.

These characteristics can also be determined empirically, from the residues $\hat{v} = y - X\hat{a}$. In AR5, chapter 10, contributors show some embarrassment and inconsistency on this subject: “It is difficult to evaluate internal variability on multi-decadal time scales (1950–2010) in observations, given the *shortness of the observational record...*” (p. 881), in contradiction with: “... it is difficult to validate climate models’ estimates of internal variability *over such a long period*” (1861–2010: p. 882.)

The second reason is that paleoclimatic data do exist, and thus cannot be ignored. Millennial observations suggest a causal relationship between solar activity and global temperature. The role of identification, as well as of D&A, is to assess the validity of this suggestion through statistical analysis. Limiting itself to a centennial time scale, the D&A leaves virtually no possibility to attribute the recent warming to solar activity rather than to human influence. On the other hand, treatment of the millennial data by D&A would almost certainly lead to conclusions similar to ours.

5.5. El Niño: a confusion factor between cause and effect

Internal variability mainly arises from Ocean chaos, through the *thermohaline circulation*, also called *meridional overturning circulation (MOC)*. The driving force of this circulation is the downwelling of the cooled and densified waters in Polar Regions. Those disperse and spread at the bottom of the oceans before resurfacing, among many others places, in the vicinity of the eastern coast of Pacific. The chaotic variations of the atmospheric circulation can inhibit for a more or less long time these cold upwelling, whose absence then

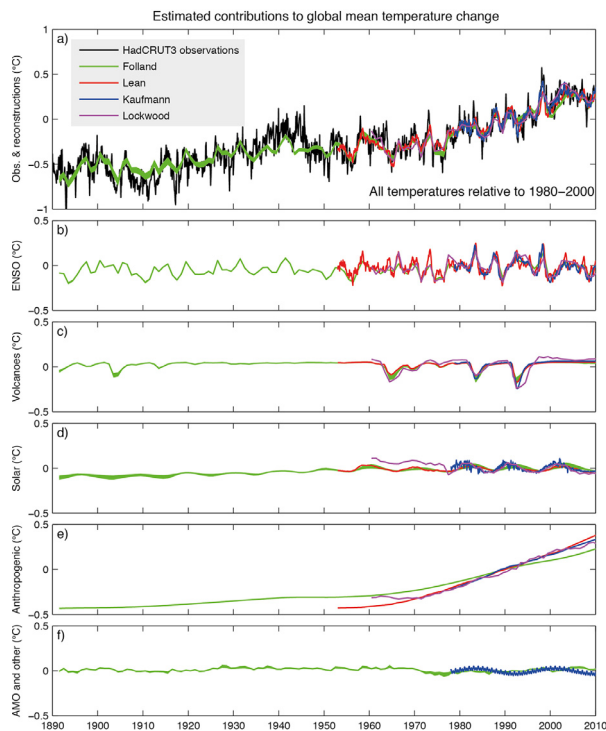


Fig. 11. From Imbers et al. (2013).

(Top) The variations of the observed global mean surface temperature anomaly (HadCRUT3), and the best multivariate fits using the method of Lean, Lockwood, Folland and Kaufmann.

(Below) The contributions to the fit from (b) El Niño–Southern Oscillation (ENSO), (c) volcanoes, (d) solar forcing, (e) anthropogenic forcing and (f) other factors (Atlantic Multi-decadal Oscillation (AMO) for Folland and a 17.5-year cycle, semi-annual oscillation (SAO), and Arctic Oscillation (AO) from Lean).

induces a more or less temporary warming. It is the El Niño phenomenon, and La Niña refers to the inverse situation.

The intensity of El Niño phenomena is assessed through the ENSO index (El Niño South Oscillation Index, or SOI), defined from a batch of measures: pressure, atmospheric and oceanic temperatures, wind speeds, etc. A strong correlation between ENSO and short-term global temperature variations is established, and makes the interest of this index.

The ENSO index is equated with an external driver in many studies: Lean (2009), Lockwood (2008), Folland et al., 2013, Kaufmann, Kauppi, Mann, & Stock (2011). Their works were collected by Imbers, Lopez, Huntingford, and Allen (2013), and reported in the AR5. Our Fig. 11 reproduces figure 10.6 of AR5. It can be criticized in several respects.

The anthropogenic contribution to global warming appears to be predominant (frame e). Among them, the lowest is that from Folland (green), which deals with the longest duration of observation (1890–2010); the others start in the 1950's or later. Visibly, the more the duration is restricted to the recent period, the more the correlation between warming and human activity predominates. Conversely, there is little doubt that an attribution based on millennial observations would reverse the findings of the D&A, in accordance with the results of the identification.

Finally, there is something more questionable: the assimilation of the ENSO index (or similar: AMO, SAO, AO) to some external forcings. Recall that these indexes consist in batches of climatic observations. Each of them is an *effect* of the external forcings, and a combination of effects cannot in any case be considered as a *cause* for the climate system as a whole. Actually, as said in 3.6, internal variability results from a tingling of elementary independent causes, but as soon as a measurable effect appears, it depends also

on the global or regional climatic state, which depends itself of the real external causes.

It is not because oceanic chaos is involved in the onset of El Niño that it is akin to an independent perturbation: the up-welling's are not only due to chance, but are modulated by the mean level of the upper thermocline limit, which mainly depends on the amount of heat in the ocean, itself determined by the radiative balance, and therefore by the external forcings. One might consider ENSO as a cause (in the sense of an external driver) only for some subsystem, to be delimited through decomposition of the climate process in interconnected sub-systems, involving various feedback loops. Hence, dealing with El Niño in the same way than an external forcing is a methodological error, which is obvious to any expert in systems science.

Yet, in AR4 (2013), IPCC quote numerous works on the dependence of ENSO on solar activity, and more generally of many other tropical Pacific climatic signals, as attested by the following quotations:

1. van Loon, Meehl, and Shea, 2007: "This then is physically consistent with the mechanisms that link solar forcing to a strengthening of the climatological mean circulation and precipitation features in the tropical Pacific";
2. van Loon and Meehl, 2008 "in solar peak years the sea level pressure (SLP) is, on average, above normal in the Gulf of Alaska and south of the equator";
3. White and Liu, 2008 "we find most El Niño and La Niña episodes from 1900–2005... Here we find these alignments replicated in both coupled general circulation model and conceptual model driven by 11-yr solar forcing";
4. Meehl, Arblaster, Matthes, Sassi, and van Loon, 2009 "One of the mysteries regarding Earth's climate system response to variations in solar output is how the relatively small fluctuations of the 11-year solar cycle can produce the magnitude of the observed climate signals in the tropical Pacific associated with such solar variability";
5. Tung and Zhou, 2010 "It is noted that previous reports of a coldtongue (La Niña-like) response to increased greenhouse or to solar-cycle heating were likely caused by contaminations due to the dominant mode of natural response in the equatorial Pacific";
6. Roy and Haigh, 2010 "An important aspect of our paper is to point out that the timing is crucial to show how this produces apparent discrepancies between different analyses and how it may be used to test mechanisms proposed to explain solar-climate links, in the context of ENSO variability";
7. Roy and Haigh (2012). Both the SLP and SST signals vary coherently with the solar cycle and neither evolves on an ENSO-like time scale;
8. Bal, Schimanke, Spanghel, and Cubasch, 2011 "there is evidence for a La Niña-like response assigned to solar maximum conditions";
9. Haam and Tung, 2012 "The solar peak years can coincide with cold ENSO by chance, even if the two time series are independent";
10. Hood and Soukharev, 2012 "the tropical lower stratospheric response is produced mainly by a solar-induced modulation";
11. Misios and Schmidt, 2012. "the tropical Pacific Ocean should warm when the sun is more active".

All the above references are quoted from AR5 (Box 10.2: *The Sun's Influence on the Earth's Climate*). They take place after the following statement: « it can be difficult to discriminate the solar-forced signal from the El Niño–Southern Oscillation (ENSO) signal ». Yet, this wording seems to go against the substance of the quoted works (except the ninth): the question is not to discriminate between two more or less similar signals, but to recognize that the

ENSO signal is not an independent external forcing, and that it is inconsistent to include it, like in Fig. 11, with the same status as the real external forcings. It has the effect of minimizing the contribution of solar activity, already underestimated by omitting the millennial observations. In contrast, the above proposed identification method clearly detects a strong contribution of solar activity in the recent climate variations.

6. Conclusions

General circulation models are powerful tools for the study of the climate system. Unfortunately, they still include many empirical representations concerning phenomena to which the climate is extremely sensitive, mainly those involved in the generation of clouds. It is also possible that some climate mechanisms be still completely unknown, in particular those related to solar activity.

These models should therefore absolutely be validated by observations. Regarding global temperatures, models must be assessed according to their ability to predict, or at least to reproduce the past evolutions. The approach by “Detection and Attribution” of the global warming is an attempt in this direction, but it not convincing for the reasons set out in Sections 5.4 and 5.5 and that we recall:

The first reason is the systematic restriction of observations to the period ‘history’ (post 1850), or even to the period ‘satellite’ (post 1979), thus leaving out paleoclimatic data, that are essential despite their imperfections.

The second is a flagrant systemic error, relative to the use of variability index (ENSO, AMO, or other). When there is confusion between cause and effect, it is difficult to give some credit to the resulting conclusions.

The third is that the findings of D&A are contradicted by those of the identification of the climate system (Sections 2 to 4). Observation data being what they are, findings of identification are far from perfect. Yet parametric confidence intervals and hypothesis testing related to identification allow direct comparison with the D&A. It appears that, despite dispersion of the observation data, the thesis of a predominant contribution of human activity to global warming should be revisited in favor of dominant natural contributions: solar activity and internal variability.

Appendix A. Three component decomposition

The decomposition of a (solar) signal y into its three components is obtained here by a Raugh-Tung-Striebel smoother (see e.g. Simo Särkkä, 2013), based on the following stochastic model:

$$\begin{aligned} y &= y_1 + y_2 + y_3, \\ dy_1^3/dt^3 &= w_1, \\ dy_2^2/dt^2 + (2\pi/11)y_2 &= w_2, \\ y_3 &= w_3, \end{aligned}$$

where the w_i are assumed Gaussian independent white noises, whose power spectra are the synthesis parameters of the algorithm.

Appendix B. Estimating the parametric uncertainty variance

Let’s explicit the dependence of the observed output y of a process in relation to a vector θ of parameters by writing:

$$y = f(\theta) + v,$$

where:

$$- y = [y_1 \cdots y_t \cdots y_N]^T \text{ is the sequence of observed outputs, from time } t=1 \text{ to } t=N$$

- $f(\theta) = [f_1(\theta) \cdots f_t(\theta) \cdots f_N(\theta)]^T$ is the series of the outputs, which would result from the simulation of the exact model driven by the observed inputs.
- $v = [v_1 \cdots v_t \cdots v_N]^T$ represents the noises and disturbances acting on the output, including those coming from input errors. This sequence is assumed to be identically distributed, ergodic and centered, but not independent.

The OE estimate of $\hat{\theta}$ is that which minimizes the criterion:

$$J(\theta) = \|y - f(\theta)\|^2.$$

Around optimal estimate, the first order development of the function $f(\theta)$ is written as:

$$f(\theta) \sim f(\hat{\theta}) + F_\theta(\theta - \hat{\theta})$$

where F_θ is the Jacobian matrix of partial derivatives of f . At the optimum, the gradient J_θ of $J(\theta)$ is zero. It develops as:

$$J_\theta = 2F_\theta^T(y - f(\hat{\theta})) = 2F_\theta^T(v + f(\theta) - f(\hat{\theta})) = 0$$

Replacing $f(\theta)$ by its development gives:

$$2F_\theta^T(v + F_\theta(\theta - \hat{\theta})) \sim 0$$

Define F_θ^+ as the pseudo-inverse of F_θ : $F_\theta^+ = (F_\theta^T F_\theta)^{-1} F_\theta^T$. Premultiplying the equation above by $(F_\theta^T F_\theta)^{-1}$ leads to the error estimation:

$$\hat{\theta} - \theta \sim F_\theta^+ v$$

The error variance $V_{\theta\theta} = E[(\hat{\theta} - \theta)(\hat{\theta} - \theta)^T]$ is therefore approximated by: $V_{\theta\theta} \sim E(F_\theta^+ v v^T F_\theta^+) = F_\theta^+ V_{vv} F_\theta^+$, where $V_{vv} = E(v v^T)$.

In order to perform this expression, the Jacobian matrix F_θ is computed through finite differences, carrying out n simulations, successively varying each component: $\hat{\theta}_i \rightarrow \hat{\theta}_i + \delta\theta_i$. Under the ergodicity hypothesis, the variance matrix V_{vv} can be calculated using the autocorrelation function of the residuals $\hat{v} = y - f(\hat{\theta})$:

$$V_{vv}(i, j) \sim \frac{1}{N} \sum_{t=1}^N \hat{v}_i \hat{v}_{t+i-j}$$

Once determined variance $V_{\theta\theta}$, one can perform any classical analyses: uncertainty ranges, parametric tests, etc.

References

SPM, Alexander, L. V., Allen, S. K., Bindoff, N. L., Bréon, F. M., Church, J. A., Cubasch, U., et al. (2013). *Summary for policymakers* (2013).
 AR5, Stocker, T. F., Qin, D., Plattner, G. K., Tignor, M., Allen, S. K., Boschung, J., et al. (2013). *Contribution of working group I to the fifth assessment report of the intergovernmental panel on climate change*.
 Åström, K. J., & Eykhoff, P. (1971). System identification – a survey. *Automatica*, 7(2), 123–162.
 Bal, S., Schimanke, S., Spanghel, T., & Cubasch, U. (2011). On the robustness of the solar cycle signal in the Pacific region. *Geophysical Research Letters*, 38, L14809.
 Clette, F., Svalgaard, L., Vaquero, J. M., & Cliver, E. W. (2015). Revisiting the sunspot number. In *The solar activity cycle* (pp. 35–103). New York: Springer.
 Crowley, T. J., & Unterman, M. B. (2013). Technical details concerning development of a 1200-yr proxy index for global volcanism. *Earth System Science Data*, 5.
 de Larminat, P. (2009). *Automatique appliquée*. Paris, Lavoisier: Wiley and Sons.
 de Larminat, P. (2014). *Climate change, identification and projections* London.
 de Larminat, P., & Thomas, Y. (1977). *Automatique des systèmes linéaires 2. Identification, Flammarion, Paris*.
 Delagey, G., & Bard, E. (2011). An Antarctic view of Beryllium-10 and solar activity for the past millennium. *Climate Dynamics*, 36(11–12), 2201–2218.
 Faivre, R., Iooss, B., Mahévas, S., Makowski, D., & Monod, H. (2013). *Analyse de sensibilité et exploration de modèles: Application aux sciences de la nature et de l’environnement* Editions Quae, Paris.
 Folland, C. K. (2013). High predictive skill of global surface temperature a year ahead. *Geophysical Research Letters*, 40, 761–767.
 Haam, E., & Tung, K. K. (2012). Statistics of solar cycle-La Niña connection: Correlation of two autocorrelated time series. *Journal of the Atmospheric Sciences*, 69, 2934–2939.
 Hasselmann, K. (1993). Optimal fingerprints for the detection of time-dependent climate change. *Journal of Climate*, 6(10), 1957–1971.

- Hegerl, G. C., Hoegh-Guldberg, O., Casassa, G., Hoerling, M. P., Kovats, R. S., Parmesan, C., et al. (2010). Good practice guidance paper on detection and attribution related to anthropogenic climate change. In Meeting report of the intergovernmental panel on climate change expert meeting on detection and attribution of anthropogenic climate change (p. 8). IPCC working group I technical support unit. Bern, Switzerland: University of Bern.
- Hegerl, G., & Zwiers, F. (2011). Use of models in detection and attribution of climate change. *Wiley Interdisciplinary Reviews: Climate Change*, 2(4), 570–591.
- Hood, L. L., & Soukharev, R. E. (2012). The lower-stratospheric response to 11-yr solar forcing: Coupling to the troposphere-ocean response. *Journal of the Atmospheric Sciences*, 69, 1841–1864.
- Imbers, J., Lopez, A., Huntingford, C., & Allen, M. R. (2013). Testing the robustness of the anthropogenic climate change detection statements using different empirical models. *Journal of Geophysical Research Atmospheres*, 118(8), 3192–3199.
- Kaufmann, R. K., Kauppi, H., Mann, M. L., & Stock, J. H. (2011). Reconciling anthropogenic climate change with observed temperature 1998–2008. *Proceeding of the National Academy of Sciences of the United States of America*, 108, 11790–11793.
- Kopp, G., & Lean, J. L. (2011). A new, lower value of total solar irradiance: Evidence and climate significance. *Geophysical Research Letters*, 38(1).
- Landau, I. D. (2001). *Identification des systèmes*. Paris: Hermès science publications.
- Lean, J. L., & Rind, D. H. (2009). How will Earth's surface temperature change in future decades? *Geophysical Research Letters*, 36, L15708.
- Lean, J. (2004). Solar irradiance reconstruction. *IGBP PAGES/World data center for paleoclimatology data contribution series # 2004-035*. NOAA/NGDC Paleoclimatology program, Boulder, CO.
- Ljung, L. (1999). *System identification: Theory for the user*.
- Ljungqvist, F. C. (2009). N. hemisphere extra-tropics 2,000 yr decadal temperature reconstruction. *IGBP PAGES/World data center for paleoclimatology data contribution series # 2010-089*. NOAA/NCDC Paleoclimatology program, Boulder, CO.
- Lockwood, M., & Frohlich, C. (2008). Recent oppositely directed trends in solar climate forcings and the global mean surface air temperature: II. Different reconstructions of the total solar irradiance variation and dependence on response time scale. *Proceeding of the Royal Society London A*, 464, 1367–1385.
- Loehle, C. (2007). A 2000-years global temperature reconstruction based on non-treering proxies. *Energy & Environment*, 18(7+8).
- Mann, Michael E., Bradley, Raymond S., & Hughes, Malcolm K. (1999). Northern hemisphere temperatures during the past millennium: Inferences, uncertainties, and limitations. *Geophysical Research Letters*, 26, 759–762.
- Meehl, G. A., Arblaster, J. M., Matthes, K., Sassi, F., & van Loon, H. (2009). Amplifying the Pacific climate system response to a small 11-747 year solar cycle forcing. *Science*, 325, 1114–1118.
- Meinshausen, M., Raper, S. C. B., & Wigley, T. M. L. (2011). Emulating coupled atmosphere-ocean and carbon cycle models with a simpler model, MAGICC6-Part 1: Model description and calibration. *Atmospheric Chemistry and Physics*, 11(4), 1417–1456.
- Misios, S., & Schmidt, H. (2012). Mechanisms involved in the amplification of the 11-yr solar cycle signal in the Tropical Pacific ocean. *Journal of Climate*, 25, 5102–5118.
- Moberg, A. (2005). 2,000-Year Northern hemisphere temperature reconstruction. *IGBP PAGES/World data center for paleoclimatology data contribution series # 2005-019*. NOAA/NGDC Paleoclimatology program, Boulder, CO.
- Roy, I., & Haigh, J. D. (2010). Solar cycle signals in sea level pressure and sea surface temperature. *Atmospheric Chemistry and Physics*, 10, 3147–3153.
- Roy, I., & Haigh, J. D. (2012). Solar cycle signals in the Pacific and the issue of timings. *Journal of the Atmospheric Sciences*, 69(4), 1446–1451.
- Särkkä, S. (2013). *Bayesian filtering and smoothing (vol. 3)*. Cambridge University Press.
- Shapiro, A. I., Schmutz, W., Rozanov, E., Schoell, M., Haberreiter, M., Shapiro, A. V., & Nyeki, S. (2011). A new approach to the long-term reconstruction of the solar irradiance leads to large historical solar forcing. *Astronomy & Astrophysics*, 529, A67.
- Söderström, T., & Stoica, P. (1988). *System identification*. Prentice-Hall, Inc.
- Tung, K.-K., & Zhou, J. (2010). The Pacific's response to surface heating in 130 yr of SST: La Niña-like or El Niño-like? *Journal of the Atmospheric Sciences*, 67, 2649–2657.
- Usoskin, I. G., Korte, M., & Kovaltsov, G. A. (2008). Role of centennial geomagnetic changes in local atmospheric ionization. *Geophysical Research Letters*, 35, L05811.
- van Loon, H., & Meehl, G. A. (2008). The response in the Pacific to the sun's decadal peaks and contrasts to cold events in the Southern Oscillation. *Journal of Atmospheric and Solar-Terrestrial Physics*, 70, 1046–1055.
- van Loon, H., Meehl, G. A., & Shea, D. J. (2007). Coupled air-sea response to solar forcing in the Pacific region during northern winter. *Journal of the Atmospheric Sciences*, 112, D02108.
- Walter, E., & Pronzato, L. (1997). *Identification of parametric models from experimental data*. Springer Verlag.
- White, W. B., & Liu, Z. Y. (2008). Non-linear alignment of El Niño to the 11-yr solar cycle. *Geophysical Research Letters*, 35, L19607.



Philippe de Larminat (Graduate Engineer, 1964, Ph. D., 1972). He was Professor at the Institut National des Sciences Appliquées (Rennes, France) and École Centrale (Nantes). He is the author of 6 books and more than 100 papers in journals and international conferences. Since 2001, he is an independent consultant and author of several patents (e.g. power plants control, satellite guidance). His research interests include mathematical modeling, system identification, signal processing and control theory. Since 2012, he conducts a pioneer work on identification of the Earth climate system.